Published in final edited form as:

Int J Mass Spectrom. 2015 February 1; 377: 699–708. doi:10.1016/j.ijms.2014.08.024.

Mass spectrometry imaging of levofloxacin distribution in TB-infected pulmonary lesions by MALDI-MSI and continuous liquid microjunction surface sampling

Brendan Prideaux[a,*], **Mariam S. ElNaggar**[b], **Matthew Zimmerman**[a], **Justin M. Wiseman**[b], **Xiaohua Li**[a], and **Véronique Dartois**[a]

[a]Public Health Research Institute, New Jersey Medical School, Rutgers, Newark, NJ 07103, USA

[b]Prosolia, Inc., Indianapolis, IN 46202-1, USA

Abstract

A multi-modal mass spectrometry imaging (MSI) and profiling approach has been applied to assess the partitioning of the anti-TB fluoroquinolone levofloxacin into pulmonary lesions. Matrix-assisted laser desorption ionization mass spectrometry imaging (MALDI-MSI) and a commercial liquid microjunction surface sampling technology (LMJ-SSP), or flowprobe, have been used to both spatially profile and image drug distributions in lung tissue sections from TB-infected rabbits following oral administration of a single human-equivalent dose.

Levofloxacin levels were highest at 6 h post-dose in normal lung, cellular granuloma, and necrotic caseum compartments. The drug accumulated in the cellular granuloma regions with lower amounts partitioning into central caseous compartments. Flowprobe imaging at 630 μm (limited by the probe tip diameter) enabled visualization of drug distribution into lesion compartments, including limited differentiation of relative drug abundance in cellular versus caseous regions of the lesions.

MALDI-MSI analysis at 75 μm provided more detailed drug distribution, which clearly accumulated in the cellular region immediately surrounding the central caseum core. Imaging and profiling data acquired by flowprobe and MALDI-MSI were validated by quantitative LC/MS/MS analysis of lung and granuloma homogenates taken from the same animals.

The results of the investigation show flowprobe imaging and sampling as a rapid and sensitive alternative to MALDI-MSI for profiling drug distributions into tissues when spatial resolution of data below the threshold of the probe diameter is not required.

Keywords

MALDI-MSI; Flowprobe; Imaging; Tuberculosis; Pharmacokinetics

[*]Corresponding author. Tel.: +1 2012818025; fax: +1 9738543160. prideabr@njms.rutgers.edu (B. Prideaux)..

1. Introduction

Mass spectrometry imaging (MSI) has been comprehensively demonstrated to be a powerful analytical technique for the localization of compounds within biological tissue sections [1–3]. It has several significant advantages to traditional whole-body autoradiography compound imaging, in that MSI does not require the synthesis of labeled compounds, which can prove costly and difficult to synthesize, and offers enhanced specificity as compounds and their metabolites are resolved through their specific mass [4]. However, WBA enables fully quantitative and (in most instances) higher spatial detail than MSI.

Of all the MS imaging modalities, MALDI has been the most applied technology for direct compound imaging in tissue [5–11]. Significant advantages include the sensitivity, potential high spatial resolutions (sub 10 μm [12]) and recently full on-tissue quantitation through the use of surface-spotted standards [13,14] or adjacently positioned spiked tissue homogenates to generate calibration curves [15]. However, the technology has a number of limitations, among which ion suppression occurring due to the inherent heterogeneity of the tissue during direct tissue analysis. The lack of a chromatographic separation step during the MALDI-MSI experiment compounds this problem as the presence of heavily abundant species such as lipids and salts can result in a marked reduction in the detected ion signal for the compound of interest. Another important consideration in the sample preparatory steps is the ability to extract the compound of interest from the tissue and into applied surface matrix crystals without losing spatial integrity due to analyte delocalization. Careful optimization of any `wet' matrix application technique must be performed as inhomogeneous extraction can lead to erroneous interpretation of ion images of drug distribution, particularly in heterogeneous tissue types such as tumors or lesions.

We have previously applied MALDI-MS imaging utilizing a QqQ mass spectrometer to image the distribution of Moxifloxacin (a synthetic broad-spectrum fluoroquinolone antibiotic) in rabbit lung biopsies from Tuberculosis (TB)-infected rabbits following oral dosing [8].

While MALDI has been the most commonly applied ionization method for drug and compound MS imaging in biological tissues, more recently, multiple alternative MS imaging modalities have emerged. Of particular interest are ambient electrospray ionization methods, which enable rapid, direct tissue imaging analysis outside of the vacuum chamber and without the requirement for time-consuming matrix application steps [16,17]. Of these techniques, Desorption Electrospray Ionization (DESI) is the most widely developed and has been applied to imaging of drugs, metabolites and lipids in a range of biological tissues [18–22]. Recently there has been increased adoption of methods for spatial profiling of analytes in tissue using liquid-microjunction based surface analysis. The in situ microextractions from these liquid microjunction surface sampling probes (LMJSSP) closely integrate sampling and ionization via liquid pumped to and aspirated away from the tissue surface prior to electrospray. The commercial and continuous iterations of these probes consist of two coaxial tubes, the internal of which is connected to the nebulizer at the site of electrospray to the MS inlet. Using the venturi created by the spray, the aspirated flow rate can be modified to balance the flow of solution pumped down the outer capillary, enabling a

constant volume at the probe tip. When brought in proximity to the surface, this volume of extraction solvent forms a liquid microjunction between probe and sample, dissolving and entraining soluble analyte in the solution to be delivered to the ionization source. The technology has been applied to multiple surface analysis applications including thin layer chromatography plates, blood spots, microbial colonies and biological tissue sections [23–27]. The distribution of sulforaphane and its glutathione and N-acetyl cysteine conjugates was determined in whole body sections from a Sulforaphane-dosed mouse by selected sampling over the entire section. Whilst not generating a whole-body chemical image, this `spatial profiling' method enabled rapid acquisition of localization information for both the drug and its metabolites without sample pre-treatment [23]. Recent enhancements include the incorporation of high-pressure liquid chromatography separation into the extraction workflow enabling isomeric drug metabolites to be resolved [28].

In this paper we present the comparative application of MALDI-MS imaging and a commercial LLMJSSP to profile and image the distribution of the fluoroquinolone antibiotic levofloxacin in lung biopsy sections from orally-dosed TB-infected rabbits. The ability of anti-TB drugs to penetrate into the pulmonary granuloma and central necrotic caseum is of critical importance as insufficient drug exposure to these areas can result in incomplete sterilization of resident bacteria and emergence of resistant mutants [29,30].

2. Method

2.1. Animal experiments and tissue collection

Experiments utilizing New Zealand White (NZW) rabbits were performed with the approval of the Institutional Animal Care and Use Committee (IACUC) of Rutgers University under assurance #A-3158-01 and protocol #13034. Female rabbits used in infection studies were housed in individual cages in a biosafety level 3 (BSL3) animal facility approved for the containment of *Mycobacterium tuberculosis* (MTB).

Aerosol infection of rabbits was performed using a BioAerosol Nebulizing Generator (BANG) nebulizer delivering 18 L/min of filtered air and 6.4 L/min of aerosol (2.5×10^6 CFU/L in phosphate-buffered saline) to the CH Technologies inhalation system (Westwood, NJ). The infection was allowed to develop for 16–21 weeks prior to drug administration, by which time numerous (>50) granulomas with diverse pathology (cellular, necrotic, caseating and fibrous) could be harvested from the lungs.

Rabbits were dosed by oral gavage with levofloxacin (Sigma, St Louis, MO) at a final concentration of 75 mg/kg, the human-equivalent dose. The animals were randomly assigned to necropsy at 2 h, 6 h or 24 h after drug administration. For MS imaging experiments, small pieces of lung tissue containing a minimum of one well-developed necrotic lesion were excised and immediately flash frozen in liquid nitrogen vapor. Samples for LC-MS/MS drug quantitation were removed and prepared as previously described [8].

All MTB infected rabbit tissues were processed in a certified BSL3 facility until the viable micro-organisms had been inactivated. Sterilization of samples for imaging studies was performed by γ-irradiation. Rabbit lung biopsies were arranged in a single vertical layer in

dry ice and exposed to γ-irradiation in a 60Co irradiator using the nearest position and all three rods until 3 MRad was delivered. The procedure was validated internally to demonstrate that all MTB bacilli are killed upon delivery of such dose of γ-rays.

2.2. Tissue sectioning and matrix application

Twelve micrometer thick tissue sections were prepared using a Leica CM1850 cryostat (Buffalo Grove, IL) and mounted onto stainless steel slides (for MALDI-MSI analysis) or frosted glass microscope slides (for flowprobe imaging, profiling and histology). After sectioning, tissue sections were immediately transferred to a −80 C freezer for storage.

Prior to MALDI-MSI analysis, tissue sections were removed from the −80 °C freezer and allowed to reach room temperature for 15 min. Three milliliter of 50% methanol containing 2 pmol/μL levofloxacin-d_3 (C/D/N Isotopes, Quebec, Canada) was applied to the surface by airspray deposition at 40 psi, followed by 25 mg/mL DHB (50% methanol, 0.1% TFA). The airbrush (Paasche Model VL, Chicago, IL) was positioned at a distance of 30 cm from the tissue and 20 passes over the tissue were performed with the tissue being allowed to fully dry between coatings. This approach was chosen as applying the internal standard independently of the matrix application has been shown to produce a more homogeneous signal for normalization purposes [31]

2.3. MALDI-MSI analysis

Optimization of MALDI Orbitrap XL instrument parameters was performed by spiking 1 μl of a 10 pmol/μL levofloxacin standard (in 50% methanol) onto the surface of 12 μm thick control rat lung sections. DHB (25 mg/mL in 50% methanol) was applied by airspray as described in the previous paragraph. Laser energy, number of laser shots, and number of microscans were selected to maximize signal to noise for the levofloxacin *m*/*z* 362.150 peak and the deuterated levofloxacin standard at *m*/*z* 365.168.

MALDI-MSI analysis was performed using a MALDI LTQ Orbitrap XL mass spectrometer (Thermo Fisher Scientific, Bremen, Germany) with a resolution of 60,000 (at *m*/*z* 400, full width half maximum (FWHM)). The resolution was sufficient to resolve the desired levofloxacin and levofloxacin-d3 peaks from background without the requirement for MS/MS and subsequent loss of signal.

Spectra were acquired in the *m*/*z* 100–650 range, using a laser energy of 7.5 μJ and 35 laser shots were fired at each position (total of 1 microscan per position). The laser step size was set at 75 μm, at which small necrotic areas within lesions could easily be resolved and no overlapping of the laser spot on adjacent acquisitions was observed. Total image acquisition times ranged between 9 (raster area 9.6 × 9.9 mm) and 19 (raster area 16 12 mm) h.

Data visualization was performed using Thermo ImageQuest software. Normalized ion images of levolfloxacin were generated by dividing levofloxacin signal (*m*/*z* 362.149 ±0.003) by levofloxacin-d_3 signal (*m*/*z* 365.168 ±0.003). Extracted ion images were interpolated using the linear interpolate function.

2.4. Flowprobe imaging analysis

The continuous in situ microextraction and electrospray ionization flowprobe source (Prosolia, Indianapolis) was mounted onto an exactive orbitrap mass spectrometer (Thermo Fisher Scientific, Waltham, MA) for ultrahigh resolution mass analysis. The flowprobe is based on liquid microjunction surface sampling technology, where an optimized extraction solvent is pumped to the probe tip which is positioned above the sample of interest while the inner coaxial electrospray capillary draws solvent away based on the venture-assisted electrospray at the mass spectrometer inlet (Fig. 1). An acidified 90:10 methanol/water mixture was pre-optimized for extraction.

Single spot, scanned profile and array, analyses were arranged using the graphical user interface of the NMotion software set up in tandem with Xcalibur to relay contact closure signals for automated data acquisition. The probe was set to extract from the surfaces for 10 s with the subsequent 20 s collected into the data file as an integrated wash step. Spectra were acquired from 100–1000 Da in positive ion mode. Imaging data was converted into the analyze format for visualization with BioMAP3x, using Firefly 2.2 for Thermo with 0.03 *m*/*z* units per mass bin, and 630 μm separating rows and columns: a no overlap/no gap surface analysis. Due to the non-destructive nature of the analysis, the same sections were stained with Hematoxylin and Eosin per standard clinical protocol.

2.5. Drug quantitation by LC-MS/MS

Naïve matrix for calibration curves was sourced from in-house MTB-infected rabbit tissues (normal lung or dissected granulomas) and gamma irradiated for handling outside of a BSL3 environment. Tissue samples were combined 1:9 with PBS buffer to form a homogenate i.e. 100 mg tissue: 900 μL PBS buffer and pulverized at a rate of 1500 RPM for 5 min using a SPEX Sample Prep Geno/Grinder 2010 (Metuchen, NJ).

Levofloxacin tissue levels were quantified by LC/MS/MS analysis following protein precipitation. Fifty microliter of homogenate was added to 450 μL of acetonitrile/methanol [1:1] containing internal standard (500 ng/mL Diclofenac) and centrifuged at 4000 rpm for 5 min at room temperature. Standards, quality control samples and blanks in the matrix of interest were used.

LC/MS/MS analysis was performed on an AB Sciex API4000 QqQ MS (Ontario, Canada) coupled to an Agilent 1260 Infinity HPLC system. Gradient elution conditions were used on a Hypersil Gold C18 2.1 × 50 mm 3 μm column (Thermo). The mobile phase A was 0.1% formic acid and the mobile phase B was 0.1% formic acid in methanol. A 2 μl injection volume was loaded onto the column at 600 μL/min.

The QTRAP 4000 was operated in MRM mode with a 100 ms dwell time and quantitation of drug levels in tissue was conducted using the transition *m*/*z* 362.0 → 318.0 for levofloxacin. Diclofenac (500 ng/mL) was used as internal standard and transition *m*/*z* 296.0 → 215.0 was monitored. Mass spectrometer source conditions were optimized for the compound. Analyst software version 1.6.2 was used to perform data processing.

3. Results and discussion

3.1. Aerosol infection of rabbits

Aerosol infection of the rabbits, followed by disease progression for 16–21 weeks, produced numerous well-developed granulomas containing cellular (macrophage- and lymphocyte-rich) and heavily necrotic (caseous) central regions. Detailed information regarding pulmonary TB lesion development and its role in TB drug discovery and development is discussed in detail by Dartois [29]. In summary, granulomas arise from the host immune response to inhaled MTB. They are initially cellular in morphology and comprised of lymphocytes, macrophages, foamy macrophages and neutrophils. At this stage they are well vascularized, facilitating drug distribution into the lesion. As the granuloma matures, it begins to necrotize from the centre outwards, and vascularization is gradually destroyed, although the fibrotic rim and cellular layer remain densely vascularized. The rabbit model of TB disease has been used in drug distribution studies because it recapitulates the diverse disease pathology seen in human TB, including advanced lesion morphology with a cellular region surrounding a necrotic or caseous center [32].

3.2. MALDI-MSI analysis

MALDI mass spectra taken from levofloxacin standard, 2 h post-dose biopsy tissue and undosed control are shown in Fig. 2. Positive mode MALDI-MS analysis of levofloxacin produces a primary $[M + H]^+$ ion at *m*/*z* 362.150 (Fig. 2A). This ion was clearly observed in the tissue section along with the externally applied standard levofloxacin-d3 at *m*/*z* 365.168 (Fig. 2B). At the selected mass resolving power of 60,000 at m/z 400 (FWHH), no interfering or overlapping background peaks were observed in the biopsy section taken from the undosed animal.

Differential distributions of levofloxacin were observed in biopsy sections at all time points analyzed (Fig. 3). The summed intensity of normalized levofloxacin signal over the entire tissue followed the 6h > 2h > 24 h order. At the earliest time point analyzed (2 h post-dose), the drug primarily accumulated in the granuloma area immediately surrounding the necrotic caseum. Fig. 4 shows an enlarged region of the MALDI-MS image with corresponding optically scanned tissue prior to matrix application and adjacent H&E stained histological reference. Penetration of levofloxacin into the caseum is occurring, but at lower levels than into the surrounding cellular area. Drug accumulation into granulomas was highest at 6 h and the drug appeared to be more homogeneously distributed throughout the cellular regions where it was accumulating in comparison to uninvolved lung tissue. Levofloxacin signal could still be observed at the 24 h time point. In agreement with the previous time points, it was observed at higher levels in the cellular lesion surrounding the caseum. The distribution data confirm our previous findings for moxifloxacin (another fluoroquinolone anti-tuberculosis compound) where we also observed accumulation of the drug within the cellular granuloma regions [8].

Cholesterol was evaluated as a marker of necrotic granuloma tissue. Neutral lipids including cholesterol, cholesterol esters (CE) and triglyceride (TAG) have been shown to be present within caseum and foamy (lipid-laden) macrophages transitioning to becoming necrotic

[33]. The dehydrated cholesterol ion ($[M + H^- H_2O]^+$) at *m/z* 369.354 strongly co-localizes with caseum and the immediately surrounding cellular lesion containing abundant foamy macrophages (Fig. 5). Fig. 5A–C shows the co-registered ion images for levofloxacin and cholesterol. The differential distributions clearly show levofloxacin accumulation in the cellular area surrounding the cholesterol-rich caseum. This ability to use cholesterol as a marker for necrotic and pre-necrotic granuloma regions – as an alternative to traditional H&E histology during a full-scan imaging experiment – enables rapid co-localization of drug and caseous foci.

3.3. Spatial profiling and imaging by flowprobe-MS

A static liquid extraction surface sampling approach has previously been applied to spatially profile drug distributions in whole body sections and the data was found to correlate well with MALDI-MSI, autoradiography and LC/MS/MS data [34]. In this experiment we applied a continuous in situ microextraction approach using the commercial flowprobe to provide relative quantitation of levofloxacin within cellular granuloma, caseum and uninvolved lung tissue on biopsy sections adjacent to those used for MALDI-MSI. After careful optimization with levofloxacin-spiked tissues, an extraction solvent system of 90:10 methanol/water containing 0.1% FA and a 10 s extraction with 20 μL/min solvent flow rate was selected.

Three serial spots were extracted from different locations within cellular, caseum or uninvolved lung for each biopsy section. The sampling locations are shown in Fig. 6 in tandem with images of the stained tissue slices following flowprobe analysis. It is notable that flowprobe analysis does not affect further processing within the analytical workflow of this sample. Areas of normal, cellular and caseum tissue were initially identified by careful examination of the optical image. However, small tissue compartments (such as small `islands' of caseum) proved difficult to resolve by use of optical scans alone, and H&E stained serial sections were required to gain a greater understanding of pathological changes occurring in the advanced lesion. Careful positioning of the probe was necessary to avoid potential crossover of signal from the cellular border into caseum and vice versa.

A chart of the resulting data is displayed in Fig. 7. In agreement with the MALDI-MSI data, the drug signals were detected in the order 6h > 2h > 24h. The levofloxacin signal was approximately twice as high at 6 h than at 2 h in both granuloma and caseum tissue. In normal lung tissue a much smaller increase in levofloxacin signals occurred between the two time-points. Significantly lower signal was detected at 24 h and no significant difference in drug partitioning was observed between lesion compartments at that time. The data was in contrast to the MALDI-MS image of an adjacent tissue section, in which higher drug signals were detected in the cellular lesion than caseum and normal lung. This may be due to placement of the probe such that granuloma and caseum were both sampled within the 600 μm sampling spot. The upper and lower sampling positions (indicated by the pink circles in Fig. 6F) are from small areas of caseum surrounded by cellular lesion. It is possible that some drug was extracted from the cellular border during sampling of the caseous spots. As shown in the MALDI imaging datasets, levofloxacin has a heterogeneous drug distribution within the tissues (even within the same cellular granuloma). Due to this heterogeneity, three

samplings per tissue compartment may not have been sufficient to provide accurate localization/quantitation at the low drug concentrations present at 24 h.

The same flowprobe extraction parameters were used to generate ion maps by surface sampling (sampling over the entire tissue section at 630 μm spacings). An automated experiment was set up to collect data from a 20 × 20 spot array (2 h post-dose tissue) or 20 × 27 spot array (24 h post-dose tissue), in which 10 s extractions were performed at each sampling position. This generated 400 and 540 files, respectively, for Firefly conversion to Analyze format with 0.03 *m*/*z* units per mass bin, and 650 μm separating rows and columns. Acquisition of the imaging datasets took 1.5–2.5 h depending upon the total number of extractions required.

Extracted ion images of levofloxacin (*m*/*z* 162.10–162.20) created in BioMAP (Novartis, Switzerland) are shown in Fig. 8. In the 2 h biopsy the drug was observed at higher levels in cellular granuloma areas than either caseum or normal lung. Given the 630 μm pixel size, we could not establish precise co-localization of the highest drug signal with the cellular rim directly surrounding the caseum, as was observed in the MALDI-MS image from the 2 h post-dose sample. Levofloxacin signals were low in the 24 h tissue. However, the distribution appeared to correlate well with the MALDI-MS image with higher levels observed in the cellular granuloma than in normal lung and little to no signal observed in the caseum. By sampling an array over the entire tissue (versus a small number of discrete extractions in specific localizations) there is less potential of acquiring a misrepresentative dataset from highly-localized `hot' or `cold' spots occurring within the tissue.

Whilst lacking the spatial resolution achievable by MALDI-MSI (up to 50 μm on the MALDI Orbitrap XL), flowprobe-MS imaging provided a rapid method for evaluating drug distribution in dosed tissue sections without the need for advanced sample preparation. It has potential for use as an alternative to MALDI for profiling or imaging drugs in tissue which may not ionize well by MALDI or may suffer severe in-source fragmentation as a result of UV laser excitation. Due to the ability of ESI to generate multiply charged ions, future application to the direct-tissue imaging of larger protein-based biopharmaceuticals is also a possibility.

The flowprobe analysis did not involve normalization of extracted drug signal to a reference standard. Tomlinson et al. recently evaluated potential ion suppression effects in static liquid-surface extraction by the incorporation of an internal standard into the solvent system used to extract a compound from lung and non-lung tissue sections [35]. They recorded reproducible extractions from both tissue types with no difference in ionization recorded between them. However, due to the vast heterogeneity observed in TB-infected lung biopsies, a suitable normalization method would minimize ion-suppression effects resulting from the different tissue compositions and enable more accurate quantitation of drug signal.

Further experiments will focus on the development and validation of a normalization method to compensate for ion suppression and surface extraction effects either by use of an internal standard (spiked into the extraction solvent) or externally applied standard (e.g. sprayed onto the tissue surface).

3.4. Levofloxacin quantitation by LC/MS/MS

The imaging and surface sampling data was validated by quantitative analysis of homogenates of dissected granulomas and normal lung tissue taken from the same animals (Fig. 9). Between six and eighteen granulomas and healthy lung samples from each animal were used. As entire granulomas (consisting of both cellular and necrotic compartments) were homogenized, sub-lesional distribution could not be quantified.

Peak levels of levofloxacin in lung and granuloma were recorded at 6 h post-dose and tissue concentrations followed the same 6h > 2h > 24 h order as observed in the MALDI-MSI and flowprobe-MS spatial profiling experiments. Mean levofloxacin levels were higher in lesions than normal lung at all three time points investigated.

Whilst the LC/MS/MS data provides full quantitation of levofloxacin in lung and lesion, the method applied in isolation is limited by the lack of sub-lesional resolution. MTB is known to be present in high numbers within the necrotic caseum [36] and determination of drug partitioning into this compartment is vital for both optimizing existing and developing novel drug regimens. If sufficiently large caseous lesions are present within the animal lungs (typically >0.8 cm) the caseum can be manually dissected out and drug levels quantified. However, in this study such lesions were not present in significant numbers. Hence, the presented quantitative LC/MS/MS data should be considered corrobative to the relatively less quantitative, but much more spatially informative MALDI-MSI, and flowprobe-MS profiling and imaging results.

4. Conclusion

A multi-modal MS approach has been successfully applied to image the distribution of levofloxacin in TB-infected rabbit lung sections. MALDI-MSI, flowprobe profiling, and imaging have been utilized to generate extracted ion images detailing localizations of the drug within normal lung, cellular granuloma and caseum. The observed tissue distribution of levofloxacin was consistent through all the applied analysis modalities. Peak levels of levofloxacin in lung and lesions were recorded at 6 h post-dose and the drug was observed to accumulate in cellular granuloma regions in comparison to normal lung and necrotic caseum. Imaging and profiling data was validated by quantitative LC/MS/MS of lung and granuloma homogenates.

MALDI-MSI produced the most spatially-detailed images and, when operated in full scan MS mode, allowed for co-localization of drug signals with endogenous markers of diseased tissue morphology. It remains the most suitable approach for finely localizing compounds in tissues with highly-heterogeneous morphology. However, acquisition on the MALDI Orbitrap is a relatively slow process with full biopsy sections requiring upwards of 15 h analysis time when imaged at <100 μm spatial resolution. Reducing the laser raster spacing to match that achievable by the flowprobe (600 μm) would vastly decrease the acquisition time, enabling images to be acquired in less than 1 h. However, only material within the dimensions of the laser spot would be ablated (approximately 50 μm diameter).

Flowprobe imaging or profiling coupled to a high mass resolving Orbitrap Q Exactive was shown to be a rapid and sensitive method for visualizing drug-distributions in tissue. Although spatial resolution capabilities are limited in comparison to established MS-imaging based approaches (such as MALDI, SIMS or DESI), the selected spatial resolution was capable of producing pharmacologically-relevant images of levofloxacin within lung and lesion compartments. The speed of analysis and lack of advanced sample processing requirements (outside of preparing tissue cryosections) make the technique a good choice for high-throughput compound imaging or profiling applications when detailed localization information is not required or when the objective is to rank-order compounds from the same class based on their relative distribution into specific tissues. Additionally, as the flowprobe utilizes ESI, it may enable imaging of compound classes that can be difficult or impossible to ionize by MALDI. Due to the analysis being conducted at atmospheric pressure, there is also potential to analyze compounds and tissues that would be prove unstable in a typical high-vacuum MALDI approach. Future work will focus on incorporating internal standards and normalization methodologies to enhance the quantitative capabilities of the technique.

Acknowledgements

This work was supported by the funds from the NIH SBIR #1R43GM108083-01, as well as Grant OPP 1066499 from the Bill and Melinda Gates Foundation, and NIH grant R01 AI111967-01. The authors also wish to acknowledge Jansy Sarathy, Paul O'Brien, Isabela Freedman and Jennifer Holloway (Public Health Research Institute, New Jersey Medical School, Rutgers. Newark, NJ) for their contribution in handling animals and biopsies. The authors also thank Laura Via and Danielle Weiner (National Institute of Allergy and Infectious Diseases, National Institutes of Health, Bethesda, MA) for γ-irradiation of the infected lung tissue samples.

References

[1]. Prideaux B, Stoeckli M. Mass spectrometry imaging for drug distribution studies. J. Proteomics. 2012; 75(16):4999–5013. [PubMed: 22842290]

[2]. Sun N, Walch A. Qualitative and quantitative mass spectrometry imaging of drugs and metabolites in tissue at therapeutic levels. Histochem. Cell Biol. 2013; 140(2):93–104. [PubMed: 23881163]

[3]. Greer T, Sturm R, Li L. Mass spectrometry imaging for drugs and metabolites. J. Proteomics. 2011; 74(12):2617–2631. [PubMed: 21515430]

[4]. Solon EG, Schweitzer A, Stoeckli M, Prideaux B. Autoradiography, MALDI-MS, and SIMS-MS imaging in pharmaceutical discovery and development. AAPS J. 2010; 12(1):11–26. [PubMed: 19921438]

[5]. Castellino S, Groseclose MR, Wagner D. MALDI imaging mass spectrometry: bridging biology and chemistry in drug development. Bioanalysis. 2011; 3(21):2427–2441. [PubMed: 22074284]

[6]. Rohner TC, Staab D, Stoeckli M. MALDI mass spectrometric imaging of biological tissue sections. Mech. Ageing Dev. 2005; 126(1):177–185. [PubMed: 15610777]

[7]. Reyzer ML, Hsieh Y, Ng K, Korfmacher WA, Caprioli RM. Direct analysis of drug candidates in tissue by matrix-assisted laser desorption/ionization mass spectrometry. J. Mass Spectrom. 2003; 38(10):1081–1092. [PubMed: 14595858]

[8]. Prideaux B, Dartois V, Staab D, Weiner DM, Goh A, Via LE, Barry CE 3rd, Stoeckli M. High-sensitivity MALDI-MRM-MS imaging of moxifloxacin distribution in tuberculosis-infected rabbit lungs and granulomatous lesions. Anal. Chem. 2011; 83(6):2112–2118. [PubMed: 21332183]

[9]. Liu X, Ide JL, Norton I, Marchionni MA, Ebling MC, Wang LY, Davis E, Sauvageot CM, Kesari S, Kellersberger KA, Easterling ML, Santagata S, Stuart DD, Alberta J, Agar JN, Stiles CD, Agar NY. Molecular imaging of drug transit through the blood-brain barrier with MALDI mass spectrometry imaging. Sci. Rep. 2013; 3:2859. [PubMed: 24091529]

[10]. Trim PJ, Henson CM, Avery JL, McEwen A, Snel MF, Claude E, Marshall PS, West A, Princivalle AP, Clench MR. Matrix-assisted laser desorption/ionization-ion mobility separation-mass spectrometry imaging of vinblastine in whole body tissue sections. Anal. Chem. 2008; 80(22):8628–8634. [PubMed: 18847214]

[11]. Marko-Varga G, Fehniger TE, Rezeli M, Döme B, Laurell T, Végvári A. lization in different lung cancer phenotypes by MALDI mass spectrometry imaging. J. Proteomics. 2011; 74(7):982–992. [PubMed: 21440690]

[12]. Römpp A, Spengler B. Mass spectrometry imaging with high resolution in mass and space. Histochem. Cell Biol. 2013; 139(6):759–783. [PubMed: 23652571]

[13]. Nilsson A, Fehniger TE, Gustavsson L, Andersson M, Kenne K, Marko-Varga G, Andrén PE. Fine mapping the spatial distribution and concentration of unlabeled drugs within tissue micro-compartments using imaging mass spectrometry. PLos One. 2010; 5(7):e11411. [PubMed: 20644728]

[14]. Takai N, Tanaka Y, Saji H. Quantification of small molecule drugs in biological tissue sections by imaging mass spectrometry using surrogate tissue-based calibration standards. Mass Spectrom. (Tokyo). 2014; 3(1):A0025. [PubMed: 24738041]

[15]. Groseclose MR, Castellino S. A mimetic tissue model for the quantification of drug distributions by MALDI imaging mass spectrometry. Anal. Chem. 2013; 85(21):10099–10106. [PubMed: 24024735]

[16]. Wu C, Dill AL, Eberlin LS, Cooks RG, Ifa DR. Mass spectrometry imaging under ambient conditions. Mass Spectrom. Rev. 2013; 32(3):218–243. [PubMed: 22996621]

[17]. Nemes P. Ambient mass spectrometry for in vivo local analysis and in situ molecular tissue imaging. Trends Analyt Chem. 2012; 34:22–34.

[18]. Liu J, Gingras J, Ganley KP, Vismeh R, Teffera Y, Zhao Z. Whole-body tissue distribution study of drugs in neonate mice using desorption electrospray ionization mass spectrometry imaging. Rapid Commun. Mass Spectrom. 2014; 28(2):185–190. [PubMed: 24338966]

[19]. Lanekoff I, Thomas M, Carson JP, Smith JN, Timchalk C, Laskin J. Imaging nicotine in rat brain tissue by use of nanospray desorption electrospray ionization mass spectrometry. Anal. Chem. 2013; 85(2):882–889. [PubMed: 23256596]

[20]. Girod M, Shi Y, Cheng JX, Cooks RG. Desorption electrospray ionization imaging mass spectrometry of lipids in rat spinal cord. J. Am. Soc. Mass Spectrom. 2010; 21(7):1177–1189. [PubMed: 20427200]

[21]. Kertesz V, Van Berkel GJ, Vavrek M, Koeplinger KA, Schneider BB, Covey TR. Comparison of drug distribution images from whole-body thin tissue sections obtained using desorption electrospray ionization tandem mass spectrometry and autoradiography. Anal. Chem. 2008; 80(13):5168–5177. [PubMed: 18481874]

[22]. Wiseman JM, Ifa DR, Zhu Y, Kissinger CB, Manicke NE, Kissinger PT, Cooks RG. Desorption electrospray ionization mass spectrometry: imaging drugs and metabolites in tissues. Proc. Nat. Acad. Sci. U. S. A. 2008; 105(47):18120–18125.

[23]. Van Berkel GJ, Kertesz V, Koeplinger KA, Vavrek M, Kong AN. Liquid microjunction surface sampling probe electrospray mass spectrometry for detection of drugs and metabolites in thin tissue sections. J. Mass Spectrom. 2008; 43(4):500–508. [PubMed: 18035855]

[24]. Walworth MJ, Stankovich JJ, Van Berkel GJ, Schulz M, Minarik S. High-performance thin-layer chromatography plate blotting for liquid microjunction surface sampling probe mass spectrometric analysis of analytes separated on a wettable phase plate. Rapid Commun. Mass Spectrom. 2012; 26(1):37–42. [PubMed: 22215576]

[25]. Hsu CC, ElNaggar MS, Peng Y, Fang J, Sanchez LM, Mascuch SJ, Møller KA, Alazzeh EK, Pikula J, Quinn RA, Zeng Y, Wolfe BE, Dutton RJ, Gerwick L, Zhang L, Liu X, Månsson M, Dorrestein PC. Real-time metabolomics on living microorganisms using ambient electrospray ionization flow-probe. Anal. Chem. 2013; 85(15):7014–7018. [PubMed: 23819546]

[26]. ElNaggar MS, Van Berkel GJ. Liquid microjunction surface sampling probe fluid dynamics: characterization and application of an analyte plug formation operational mode. J. Am. Soc. Mass Spectrom. 2011; 22(10):1737–1743. [PubMed: 21952887]

[27]. Van Berkel GJ, Kertesz V. Application of a liquid extraction based sealing surface sampling probe for mass spectrometric analysis of dried blood spots and mouse whole-body thin tissue sections. Anal. Chem. 2009; 81(21):9146–9152. [PubMed: 19817477]

[28]. Kertesz V, Van Berkel GJ. Liquid microjunction surface sampling coupled with high-pressure liquid chromatography–electrospray ionization-mass spectrometry for analysis of drugs and metabolites in whole-body thin tissue sections. Anal. Chem. 2010; 82(14):5917–5921. [PubMed: 20560529]

[29]. Dartois V. The path of anti-tuberculosis drugs: from blood to lesions to mycobacterial cells. Nat. Rev. Microbiol. 2014; 12(3):159–167. [PubMed: 24487820]

[30]. Kjellsson MC, Via LE, Goh A, Weiner D, Low KM, Kern S, Pillai G, Barry CE III, Dartois V. Pharmacokinetic evaluation of the penetration of antituberculosis agents in rabbit pulmonary lesions. Antimicrob. Agents Chemother. 2012; 56(1):446–457. [PubMed: 21986820]

[31]. Pirman DA1, Kiss A, Heeren RM, Yost RA. Identifying tissue-specific signal variation in MALDI mass spectrometric imaging by use of an internal standard. Anal. Chem. 2013; 85(2): 1090–1096. [PubMed: 23214468]

[32]. Kaplan, G.; Tsenova, L. 2011, Pulmonary tuberculosis in the rabbit. In: Leong, FJ.; Dartois, V.; Dick, T., editors. A Color Atlas of Comparative Pathology of Pulmonary Tuberculosis. CRC Press; Boca Raton, FL: 2014. p. 107-130.

[33]. Kim MJ, Wainwright HC, Locketz M, Bekker LG, Walther GB, Dittrich C, Visser A, Wang W, Hsu FF, Wiehart U, Tsenova L, Kaplan G, Russell DG. Caseation of human tuberculosis granulomas correlates with elevated host lipid metabolism. EMBO Mol. Med. 2010; 2(7):258–274. [PubMed: 20597103]

[34]. Eikel D, Vavrek M, Smith S, Bason C, Yeh S, Korfmacher WA, Henion JD. Liquid extraction surface analysis mass spectrometry (LESA-MS) as a novel profiling tool for drug distribution and metabolism analysis: the terfenadine example. Rapid Commun. Mass Spectrom. 2011; 25(23):3587–3596. [PubMed: 22095508]

[35]. Tomlinson L, Fuchser J, Fütterer A, Baumert M, Hassall DG, West A, Marshall PS. Using a single, high mass resolution mass spectrometry platform to investigate ion suppression effects observed during tissue imaging. Rapid Commun. Mass Spectrom. 2014; 28(9):995–1003. [PubMed: 24677520]

[36]. Driver ER, Ryan GJ, Hoff DR, Irwin SM, Basaraba RJ, Kramnik I, Lenaerts AJ. Evaluation of a mouse model of necrotic granuloma formation using C3HeB/FeJ mice for testing of drugs against *Mycobacterium tuberculosis*. Antimicrob. Agents Chemother. 2012; 56(6):3181–3195. [PubMed: 22470120]

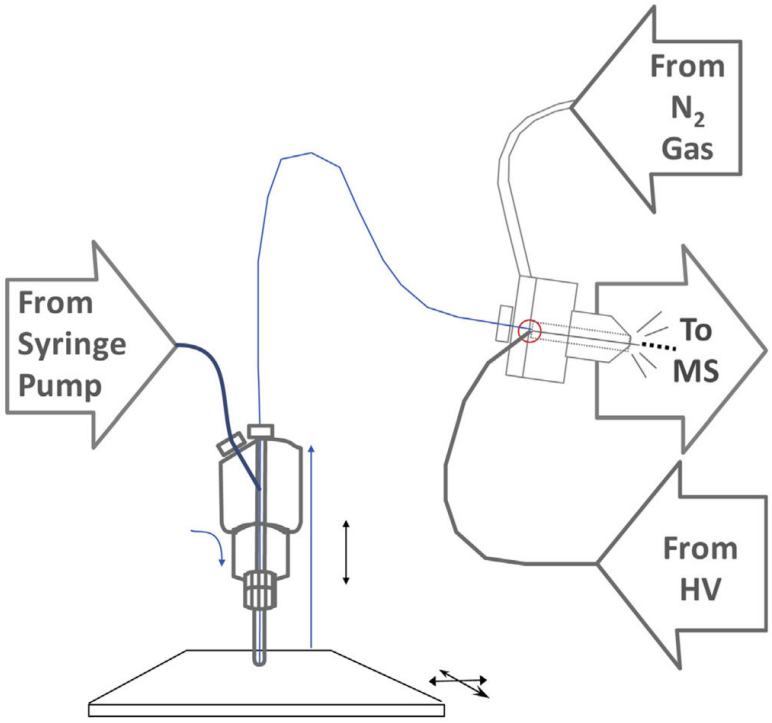

Fig. 1.

Schematic of the flowprobe device. Gas and voltage are applied at the sprayer end of the system to generate both an electrospray and venturi-induced pressure drop resulting in aspiration of solvent at a rate matched to that of the extraction solvent pumped into the probe.

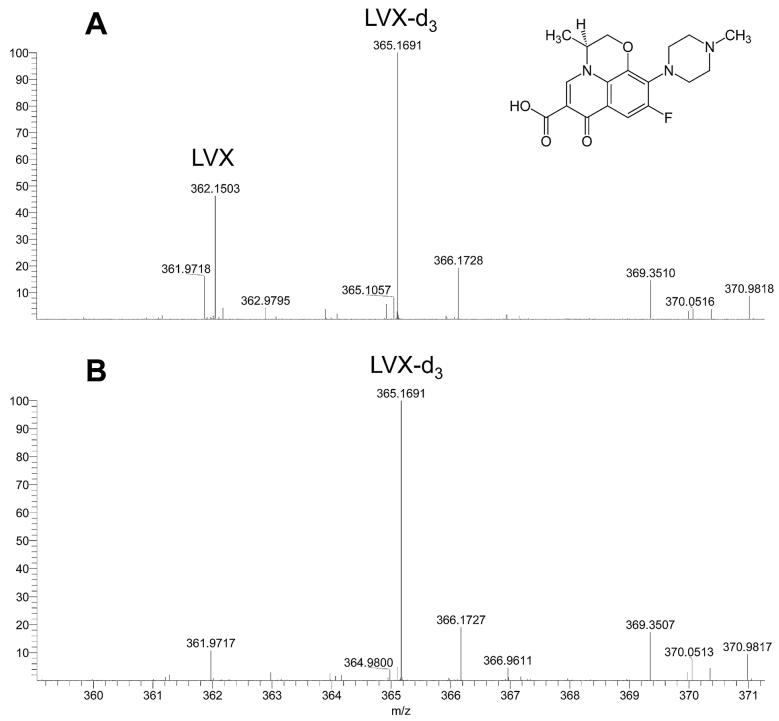

Fig. 2.

MALDI mass spectra averaged from a section taken from a 2 h post dose tissue (A) and undosed control (B). The $[M + H]^+$ levofloxain ion at *m/z* 362.150 is clearly detected in the dosed tissue and absent in the control. Levofloxacin-d_3 (applied to the tissue as internal standard) is observed in both spectra at *m/z* 365.169. The structure of levofloxacin is shown in the inset figure.

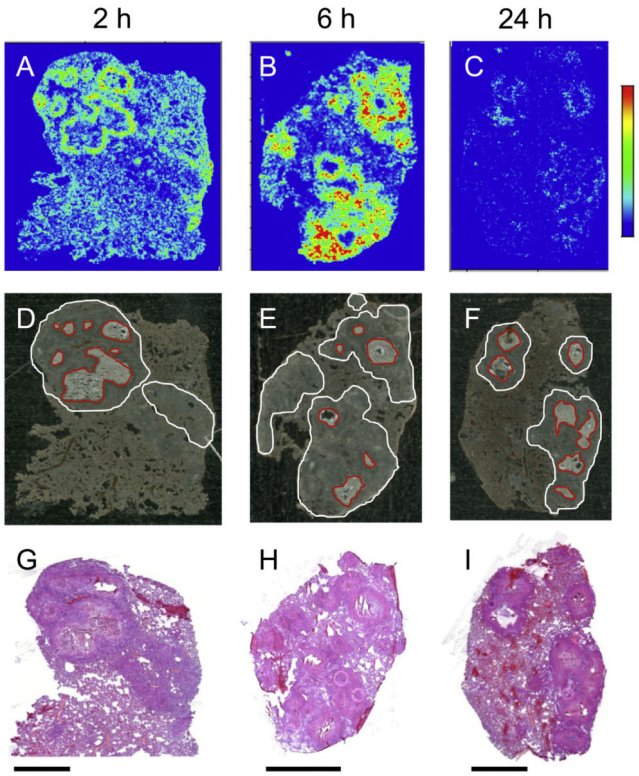

Fig. 3.

MALDI-MS images showing levofloxacin distributions within dosed tissues at 2, 6 and 24 h post-dose (A–C). The same tissue sections prior to matrix application are shown in D–F, areas of cellular lesion are outlined in white and central caseous regions are highlighted in red. Adjacent H&E-stained reference sections are shown in G–I, in which cellular granuloma tissue stains red/purple and caseum light red/pink. The highest levofloxacin signals are observed in the 6 h tissue. The drug is accumulating in the cellular region of the granuloma in the area immediately surrounding the central caseum. Scale bar = 5 mm. (For interpretation of the references to colour in this figure legend, the reader is referred to the web version of this article.)

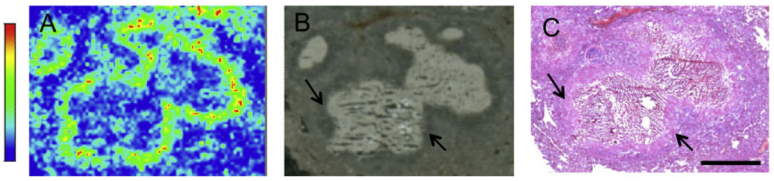

Fig. 4.

Close up of levofloxacin distribution at 2 h post-dose. The granuloma contains a large area of central caseum around which the drug is observed to accumulate. The highest signals correlate to the thin layer of cellular tissue (marked by black arrowheads in B and C) which appears darker in the optical scanned image (B) and dense pink in the adjacent H&E stained reference (C). Scale bar = 1 mm. (For interpretation of the references to colour in this figure legend, the reader is referred to the web version of this article.)

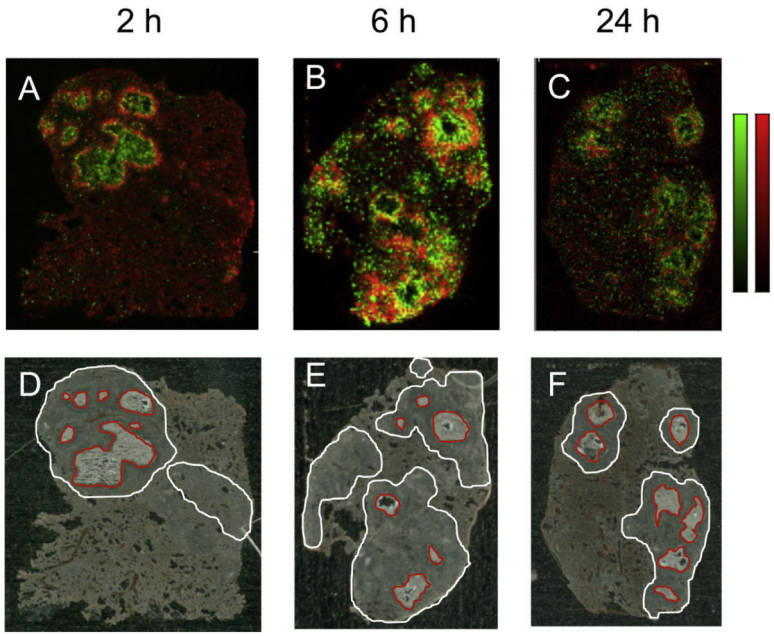

Fig. 5.

Co-localization of levofloxacin with cholesterol as a marker of necrotic tissue. Intense cholesterol signals ($[M + H^- \cdot H_2O]^+$) were recorded in the necrotic, caseous granuloma compartments (green signal in A–C). Levofloxacin signal is shown in red and overlapping regions appear yellow. Optical scans of the same tissue sections prior to matrix application are shown in D–F; areas of cellular lesion are outlined in white and central caseous regions are highlighted in red. (For interpretation of the references to colour in this figure legend, the reader is referred to the web version of this article.)

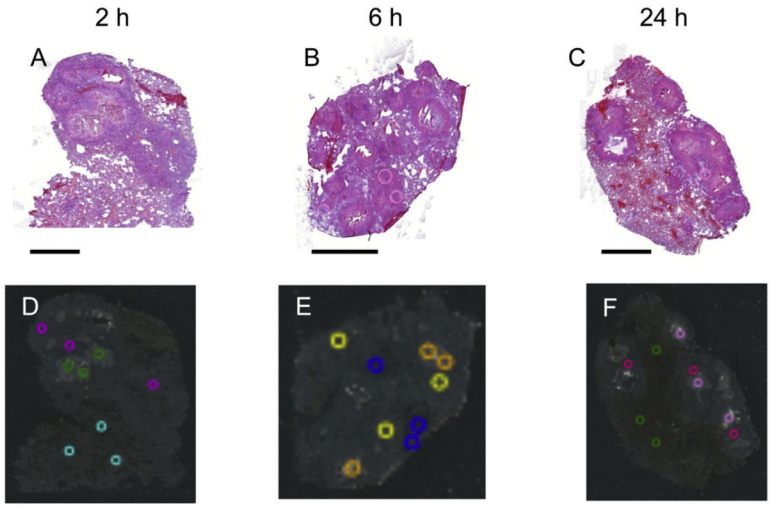

Fig. 6.

Tissue areas selected for surface sampling by flowprobe. Three discrete analyses were performed in normal lung, granuloma, and caseum on each tissue section resulting in a total of 9 extractions per tissue. Sampling positions are displayed in D–F. Normal lung: light blue in D, dark blue in E and green in F; cellular granuloma: purple in D, yellow in E and red in F; caseum: green in D, orange in E and pink in F. Scale bar = 5 mm.(For interpretation of the references to colour in this figure legend, the reader is referred to the web version of this article.)

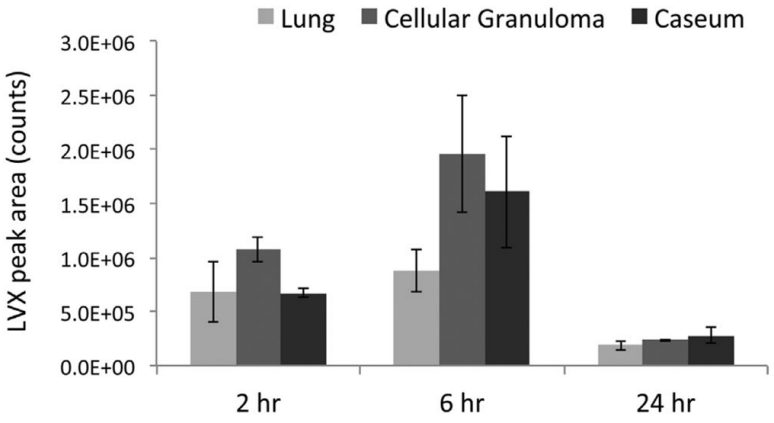

Fig. 7.

Mean levofloxacin ion counts from flowprobe analysis of rabbit lung tissue sections. The highest levels of levofloxacin were observed at 6 h post-dose. The drug was observed to accumulate within cellular granuloma at the 2 and 6 h time-points with lower levels partitioning into the caseum. $n = 3$.

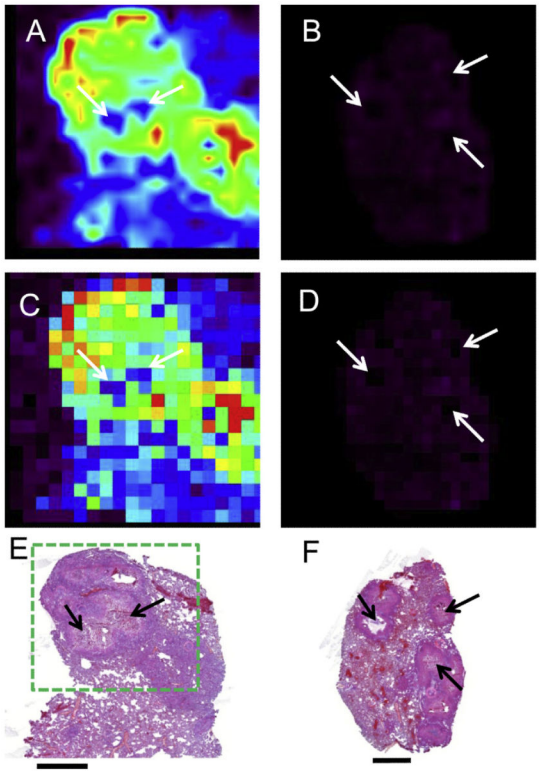

Fig. 8.

Flowprobe imaging of tissues obtained at 2 h (A) and 24 h (B) post-dose from infected rabbits dosed with levofloxacin. Interpolated images, created using the interpolation function within BioMap software, are shown in A and B. Raw images are shown in C and D. H&E-stained tissues for 2 h (E) and 24 h (F) are provided for reference. The sampling area used to construct the flowprobe images shown in A and C is outlined in green. The arrowheads point to the caseous granuloma regions. Scale bar = 5 mm. (For interpretation of the references to colour in this figure legend, the reader is referred to the web version of this article.)

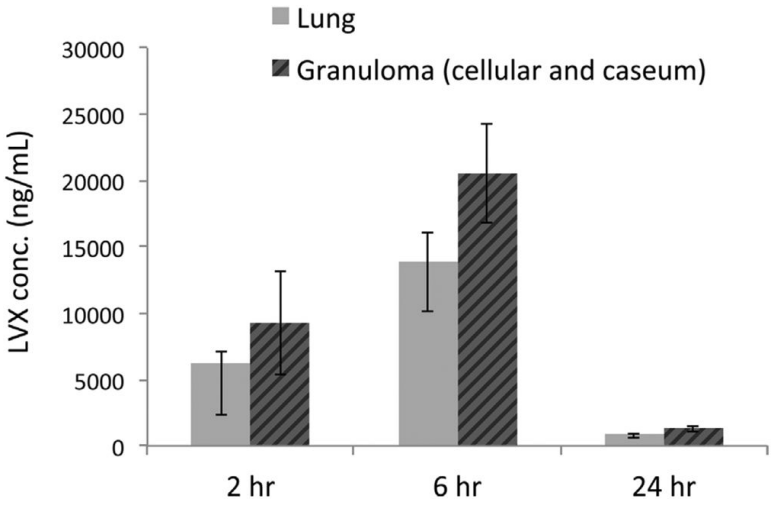

Fig. 9.

Graph showing the concentrations of levofloxacin within normal lung and homogenized granuloma (unresolved for caseum and cellular material) as determined by LC/MS/MS. In agreement with the flowprobe data, the highest levels of levofloxacin were observed at 6 h post-dose and the drug was observed to accumulate within cellular granuloma at the 2 and 6 h time-points with lower levels partitioning into the caseum. n = 6–18.